Geophysical Research Letters

RESEARCH LETTER
10.1029/2020GL088506

Key Points:
- The energy flux equator and the ITCZ are not colocated in the observed seasonal cycle
- The breakdown of this relationship is due to changes in the bottom heaviness of vertical motions
- This is especially evident in the Eastern Pacific and is related to the spatial distribution of sea surface temperatures

Supporting Information:
- Supporting Information S1

Correspondence to:
H.-H. Wei,
hohsuan.wei@colorado.edu

Citation:
Wei, H.-H., & Bordoni, S. (2020). Energetic Constraints on the intertropical convergence zone position in the observed seasonal cycle from Modern-Era Retrospective analysis for Research and Applications, Version 2 (MERRA-2). *Geophysical Research Letters*, *47*, e2020GL088506. https://doi.org/10.1029/2020GL088506

Received 28 APR 2020
Accepted 2 AUG 2020
Accepted article online 10 AUG 2020

Energetic Constraints on the Intertropical Convergence Zone Position in the Observed Seasonal Cycle From Modern-Era Retrospective Analysis for Research and Applications, Version 2 (MERRA-2)

Ho-Hsuan Wei[1,2] **and Simona Bordoni**[1,3]

[1]Division of Geological and Planetary Sciences, California Institute of Technology, Pasadena, CA, USA, [2]University of Colorado Boulder/Cooperative Institute for Research in Environmental Sciences, Boulder, CO, USA, [3]Department of Civil, Environmental and Mechanical Engineering, University of Trento, Trento, Italy

Abstract Idealized simulations show that the approximate colocation between the ITCZ and the energy flux equator (EFE), which holds on the annual and zonal average, breaks down on subseasonal timescales, as the Hadley cell develops a shallow return flow and negative gross moist stability (GMS). Here, we explore if similar mechanisms are seen in reanalysis data. In the zonal mean, a temporal offset exists between the ITCZ and the EFE as the ITCZ is retreating from the Northern to Southern Hemisphere and the Hadley cell transports energy northward across the equator despite a northward-shifted ITCZ. At these times, the southern cell has a bottom-heavy structure, with a distorted cell boundary and northward energy transport. In the Eastern Pacific, while bottom-heavy structures exist throughout the year, the bottom heaviness is stronger in boreal fall, when GMS is negative, and SSTs are weak while their Laplacian is large and negative below the ITCZ.

Plain Language Summary The intertropical convergence zone (ITCZ) is a narrow band of intense rainfall near the equator. What controls the position of the ITCZ on different timescales is a question that remains open in the literature. In the past decade, it has been argued that the tropical overturning circulation transports energy away from the ITCZ and, hence, the annual and zonal mean ITCZ is approximately colocated with the latitude at which the energy transport vanishes (the energy flux equator, EFE). Idealized numerical simulations, however, show that this relationship might break down on subseasonal timescales. Here, we use reanalysis data to explore if and why this also happens in the observed seasonal cycle. We find that in the zonal mean, the EFE and the ITCZ are located on opposite sides of the equator in boreal fall and winter, with the cross-equatorial southern Hadley circulation having a bottom-heavy structure that favors energy transport in the direction of the lower-level flow, and hence into rather than away from the ITCZ. In the Eastern Pacific, bottom-heavy circulation profiles persist throughout the year but are stronger when the ITCZ and the EFE are in opposite hemispheres and when the meridional curvature of the SST distribution is large.

1. Introduction

In the past decade, energetic arguments have provided important insights into the dynamics of the ITCZ and its position (e.g., Bischoff & Schneider, 2014; Donohoe et al., 2013; Frierson & Hwang, 2012; Hwang et al., 2013; Kang et al., 2008, 2009). Embedded in the ascending branch of the Hadley cell, the ITCZ is in this framework interpreted as part of the global energy budget: in response to a local or remote perturbation, the energetically direct Hadley cell restores energy balance by shifting its ascending branch, and with it the ITCZ, into the hemisphere with net energy input, so to transport energy across the equator into the opposite hemisphere in the direction of its upper branch. The anticorrelation between the ITCZ position and the cross-equatorial energy transport emphasized by this framework (e.g., Donohoe et al., 2013; McGee et al., 2014) rests on two assumptions: (1) the gross moist stability (GMS), that is, the efficiency with which the Hadley cell transports energy, does not change substantially and remains always positive, implying energy transport in the direction of the upper-level flow; (2) the ITCZ position is approximately colocated with the energy flux equator (EFE), that is the latitude of vanishing meridional energy transport (e.g., Kang et al., 2008). Recent studies have however highlighted how the GMS cannot always be assumed as

constant and that its changes need to be accounted for to understand the response of annual mean tropical precipitation to radiative or surface flux perturbations (Feldl & Bordoni, 2016; Merlis et al., 2013; Rencurrel & Rose, 2020; Seo et al., 2017). Additionally, idealized simulations with a seasonal cycle show limitations of the energetic constraints when ITCZ instraseasonal migrations are considered (Wei & Bordoni, 2018). More specifically, the EFE, whose position is primarily determined by the insolation forcing, always leads the ITCZ, whose location is in phase with the lower-level temperature and near-surface moist static energy (MSE). As a result, the EFE and the ITCZ do not always reside on the same side of the equator, and the GMS of the Hadley cell in which the ITCZ is embedded can become negative. This is achieved through the development of a shallow return flow near the levels of minimum MSE (Wei & Bordoni, 2018). ITCZ seasonal excursions uncorrelated with changes in cross-equatorial energy transport are also seen in aquaplanet simulations with comprehensive GCMs (Biasutti & Voigt, 2020) in the Tropical Rain belts with an Annual cycle and a Continent Model Intercomparison Project (TRACMIP) archive (Voigt et al., 2016). Because of the lack of zonal and hemispheric asymmetries and dynamical coupling with the ocean in these simulations, the extent to which these mechanisms might be an artifact of the simplified configuration and might in fact be relevant for the observed seasonal cycle remains unclear.

Reanalysis data have been used extensively in the literature to understand the energy balance of the climate system and to infer the required atmospheric and oceanic energy transport (e.g., Trenberth & Caron, 2001). Recent work has also explored observed relationships between the ITCZ and energetic diagnostics in reanalyses, both in the annual mean and in the seasonal cycle (e.g., Adam et al., 2016a, 2016b; Donohoe et al., 2013, 2014; Frierson et al., 2013). Importantly, Adam et al. (2016a, 2016b) show that a lag exists between the EFE and the ITCZ, but the implications of this lag for the energy transport by the Hadley circulation and changes in its vertical structure (and possibly GMS) have not been explored. It is, for instance, well documented that shallow circulations which import MSE exist throughout the year over the Eastern Pacific (e.g., Back & Bretherton, 2006, 2009; Zhang et al., 2004), but no study has so far investigated their relationship and influence on the ITCZ seasonal migrations. This is indeed the goal of this study: by using MERRA-2 reanalysis, we document the relationship between the ITCZ position, the EFE, the overturning circulation vertical structure, and the associated energy transport in the course of the observed seasonal cycle, both in the zonal mean and the Eastern Pacific sector. We also compare our results with those existing in the literature based on other reanalysis products, and highlight how existing residuals in the mass and MSE budgets might affect the interpretation of emerging results.

2. Data and Methods

We use fields from NASA's Modern-Era Retrospective analysis for Research and Applications, Version 2 (MERRA-2) (e.g., Bosilovich et al., 2015; Rienecker et al., 2011), with horizontal resolution of 0.5° (latitude) × 0.625° (longitude) and 3-hourly (atmospheric fields) and 1-hourly (other variables such as surface fluxes and radiation) temporal resolution for years 2002–2016. All data are averaged over 5 days (for a total of 73 pentads) for each year and then multiyear pentad means are computed. The dry mass budget in MERRA-2, like in other reanalyses, is not closed. As discussed in Trenberth (1991), a barotropic wind adjustment $\mathbf{v_c}$ hence needs to be performed to close it (Text S1 in the supporting information).

The mass adjustment is calculated from 6-hourly data on pressure levels (42 layers), which allows us to compute the vertically integrated total MSE flux at pentad temporal resolution. In Figure S1, we show how the mass adjustment significantly reduces the residual of the dry mass budget (M_dRES) over monthly timescales. This also reduces significantly the residual in the MSE budget (Figures S2a–S2c).

Despite this much smaller residual in the MSE budget, it is found that this adjustment results in a zero cross-equatorial atmospheric energy transport in the annual and zonal mean (Figure S3a). This is at odds with results reported elsewhere in the literature and theoretical arguments that relate the northward shifted position of the ITCZ to southward cross-equatorial energy transport (e.g., Adam et al., 2016a; Frierson et al., 2013; Marshall et al., 2013; Schneider et al., 2014). We therefore perform a barotropic adjustment on the MSE budget, following Hill et al. (2017) (Text S2). This better closes the MSE budget (Figures S2a and S2d) and yields a southward annual and zonal mean energy transport in agreement with other studies (Figure S3b). All analyses shown below are hence based on the MSE budget adjusted data.

In addition to more standard fields, we also compute the GMS of the zonally averaged and sector-mean overturning circulation as the efficiency of energy transport per unit mass flux (e.g., Feldl & Bordoni, 2016;

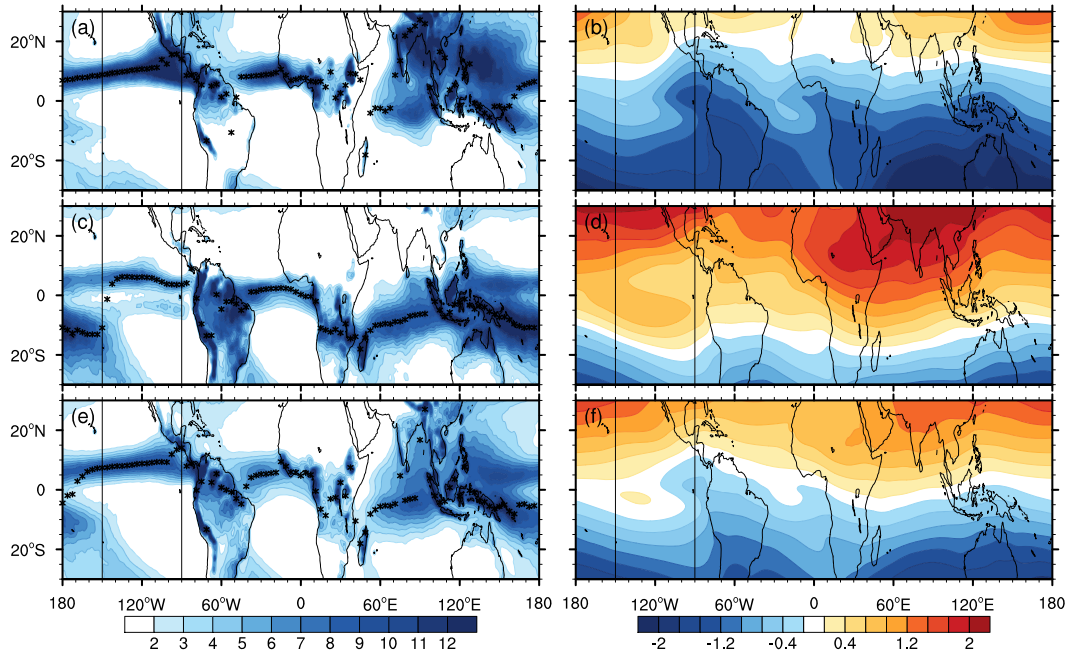

Figure 1. (a) JAS, (c) JFM, and (e) annual mean precipitation from MERRA-2 reanalysis data averaged over the years 2002–2016 (mm day^{-1}). Asterisks show the ITCZ position ($\phi_{P_{max,smth}}$; see the Supporting Information for further details on the specific ITCZ metric used). (b, d, f) Same seasonal mean as (a, c, e), but for the divergent component of the vertically integrated meridional MSE flux (10^8 W m^{-1}). The white shading represents where the meridional MSE flux vanishes, that is, the EFE. Black vertical lines indicate the Eastern Pacific sector.

Frierson, 2007; Hill et al., 2015; Kang et al., 2009; Rencurrel & Rose, 2020) to explore if and when the assumption of positive GMS breaks down. See Text S4 for more details.

3. ITCZ, Circulation, and Energy Flux

Figure 1 shows the precipitation and energy flux distribution in the tropics for Northern Hemisphere (NH) summer (July–September, JAS), winter (January–March, JFM), and in the annual mean. While both the EFE and the ITCZ tend to migrate northward (southward) in the NH summer (winter) relative to their annual mean position at every longitude, they are not colocated. Strong zonal variations are also seen in both their seasonal and annual means. For example, over the Eastern Pacific, the ITCZ remains in the NH even during NH winter, with the development of a secondary ITCZ south of the equator. Over India and Africa, the regional ITCZs more clearly follow the seasonal cycle of insolation, with excursions across the equator into the summer hemispheres. Note however how near-equatorial precipitation over the Southern Indian Ocean is evident even during NH summer, when the most active convection is found over Southeast Asia as the monsoon develops there. Over the Western Pacific, on the other hand, strong convection develops over the warm pool and over the Southern Pacific convergence zone (SPCZ) in the Southern Hemisphere (SH). The latter is particularly strong in SH summer.

The EFE also shows strong zonal asymmetries, with times during the seasonal cycle at which the energy transport vanishes at two different latitudes for a given longitude. As discussed in Bischoff and Schneider (2016) and Adam et al. (2016b), these EFE bifurcations occur over latitudes where the net energy input into the atmospheric column—the difference between top-of-atmosphere radiative fluxes and surface radiative and turbulent enthalpy fluxes—becomes negative (i.e., where there is convergence of MSE flux). Interestingly, EFE bifurcations do not always correspond to ITCZ bifurcations (or a double ITCZ), nor do their latitudes feature a clear colocation with the latitudes of the double ITCZ. For instance, in the annual mean, the EFE features two nodes north and south of the equator at 120°W. Yet, there is a single ITCZ north of the equator at that longitude. We next detail the seasonal evolution of both zonal mean and sector-mean quantities. Please note that the vertically integrated MSE flux we show here is the divergent component of the flux, which is more closely related to precipitation.

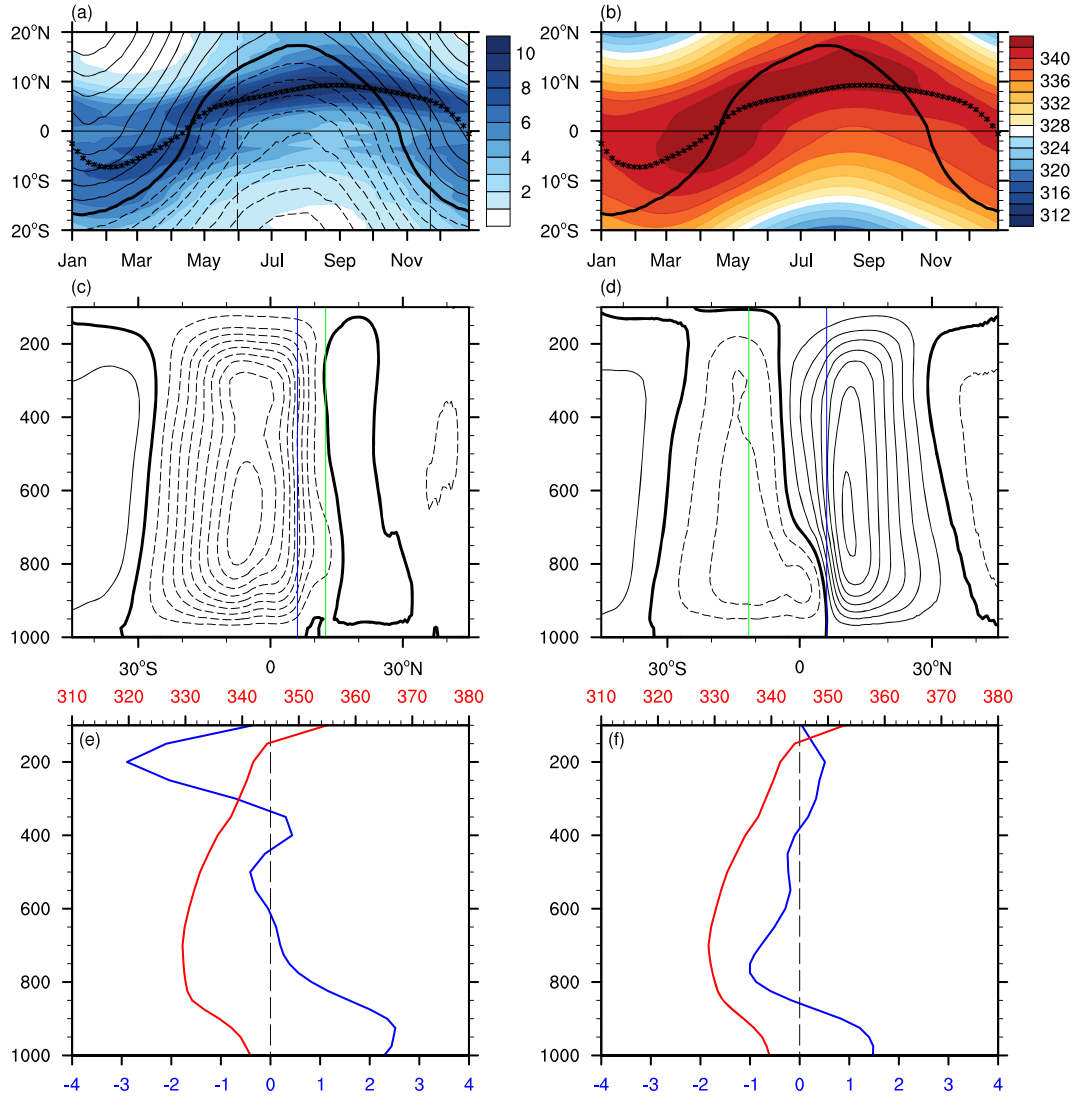

Figure 2. Seasonal evolution of (a) zonal mean precipitation (shading, mm day^{-1}) and vertically integrated meridional MSE flux (contours, W m^{-1}). Solid (dashed) contours indicate positive (negative) values and thick black contour the zero value (i.e., the EFE). The contour spacing is 2×10^7 W m^{-1}. Black vertical dashed lines indicate the two pentads used for panels (c)–(f). (b) Seasonal evolution of zonal mean MSE (K) at the lowest model level ($\sigma = 0.985$). The thick black contour indicates the EFE as in (a). The asterisks in (a, b) are the ITCZ location ($\phi_{P_{max,smth}}$). (a, b) The time evolution shown is a 9-pentad running mean. (c, d) Meridional mass streamfunction (contour, interval 2×10^{10} kg s^{-1}, positive [negative] value corresponding to clockwise [counter-clockwise] circulation) for (c) 31 May to 4 June an d (d) 22–26 November. Solid (dashed) contours indicate positive (negative) values and thick black contours the zero value. Blue vertical line indicates the $\phi_{P_{max,smth}}$ and the green vertical line the location of the EFE. (e, f) Vertical profiles of the zonal mean MSE (red, K) and meridional wind (blue, m s^{-1}) at the equator on (e) 31 May to 4 June and (f) 22–26 November.

3.1. Zonal Mean

In the zonal mean, as well documented by many previous studies, the ITCZ migrates seasonally between the two hemispheres and in the annual mean is located at around 6°N, as diagnosed from the latitude of maximal precipitation. The ITCZ location, $\phi_{P_{max,smth}}$ (defined here following the metric in Adam et al., 2016a; see Text S3), resides longer in the NH and migrates somewhat rapidly into the SH around January (Figure 2a). This results from a strengthening of the SPCZ in the Western Pacific, the development of the SH ITCZ in the Eastern Pacific, and a southward shift into the SH of the ITCZ in the African and Indian sectors.

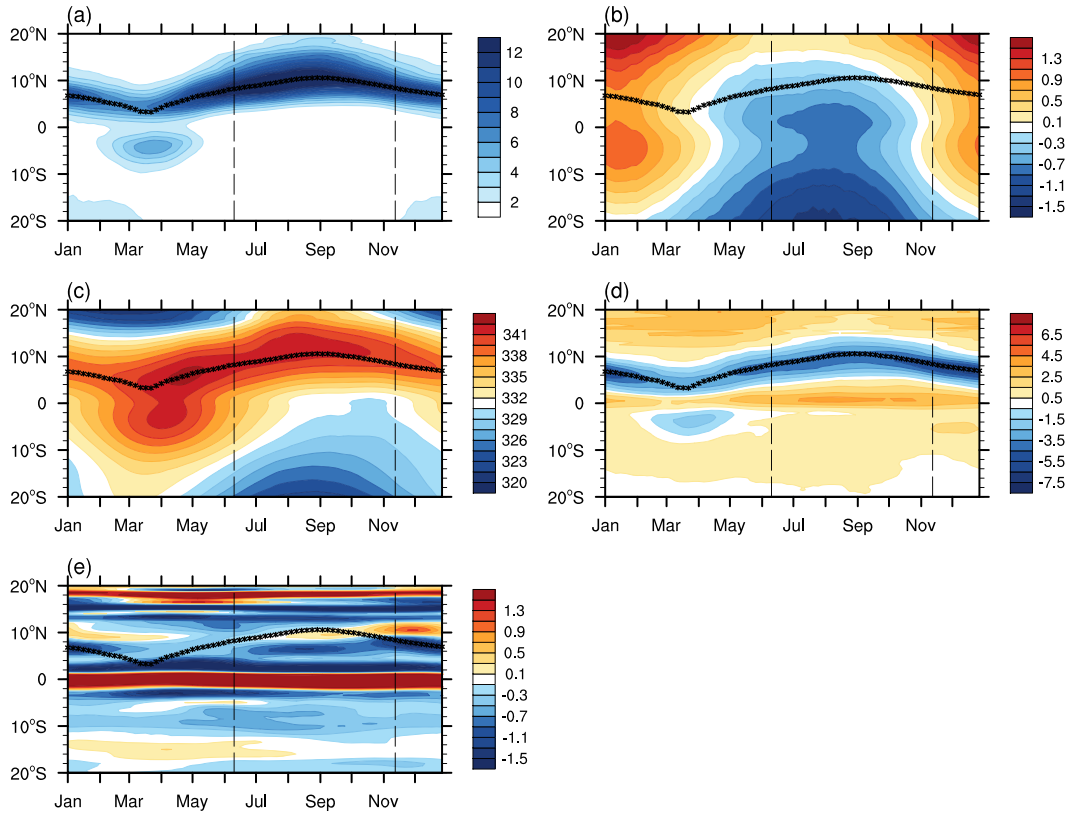

Figure 3. Seasonal evolution of zonal mean (a) precipitation (mm day^{-1}), (b) meridional MSE flux (10^8 W m^{-1}), (c) surface MSE (K), (d) lower-level (10 m) horizontal wind divergence (10^{-6} s^{-1}), and (e) meridional Laplacian of the skin temperature (10^{-11} K m^{-2}) in the Eastern Pacific sector (150°W to 90°W). The black vertical dashed lines indicate the two pentads (15–19 June and 17–21 November, respectively) used in Figure 4. The asterisks are $\phi_{P_{max,smth}}$. The time evolution shown is a 9-pentad running mean.

The ITCZ generally coevolves with the zonal mean near-surface MSE maximum and is located slightly equatorward of it (Figure 2b), consistent with convective quasi-equilibrium theories (e.g., Emanuel, 1995; Privé & Plumb, 2007). It is interesting to note how the evolution of the zonal mean MSE maximum results from a combination of temperature and moisture, with temperature maximizing further poleward than both moisture and MSE during NH summer because of the presence of land masses (Figures S4a, S4c, and S4e). The offset between temperature and moisture disappears when we only take a zonal mean over ocean (Figures S4b, S4d, and S4f), where the near-surface moisture tracks closely the near-surface temperature.

While tropical precipitation is dictated by the surface thermodynamics, remaining in the NH for a large portion of the seasonal cycle, the EFE follows the seasonal evolution of solar insolation and spends almost equal amounts of time in the two hemispheres. Unlike what was seen in the idealized simulations of Wei and Bordoni (2018), in the observations, the temporal relationship between the EFE and the ITCZ cannot simply be described as a lag, because the ITCZ evolution differs from an annual harmonic (Figures 2a and 2b).

This temporal and spatial offset between the EFE and the ITCZ raises the question of how the overturning cell in which the ITCZ is embedded might achieve negative GMS over the regions between the EFE and the ITCZ. In fact, at any time at which the EFE and the ITCZ reside on opposite sides of the equator, the cross-equatorial overturning cell transports energy in the direction of its lower branch, importing rather than exporting MSE into its ascending branch (Figure S6a). We therefore select two pentads with the same ITCZ location but different EFEs at which the southern cell is expanding into and retreating from the NH, respectively (vertical dashed lines in Figure 2a, around 31 May to 4 June and 22–26 November), and compare the associated circulation structure. The overturning circulation and the corresponding vertical profiles of meridional wind and MSE at the equator are shown in Figures 2c–2f. Other than being much weaker than the winter cell in its expanding phase, the retreating cell is much broader at lower levels than

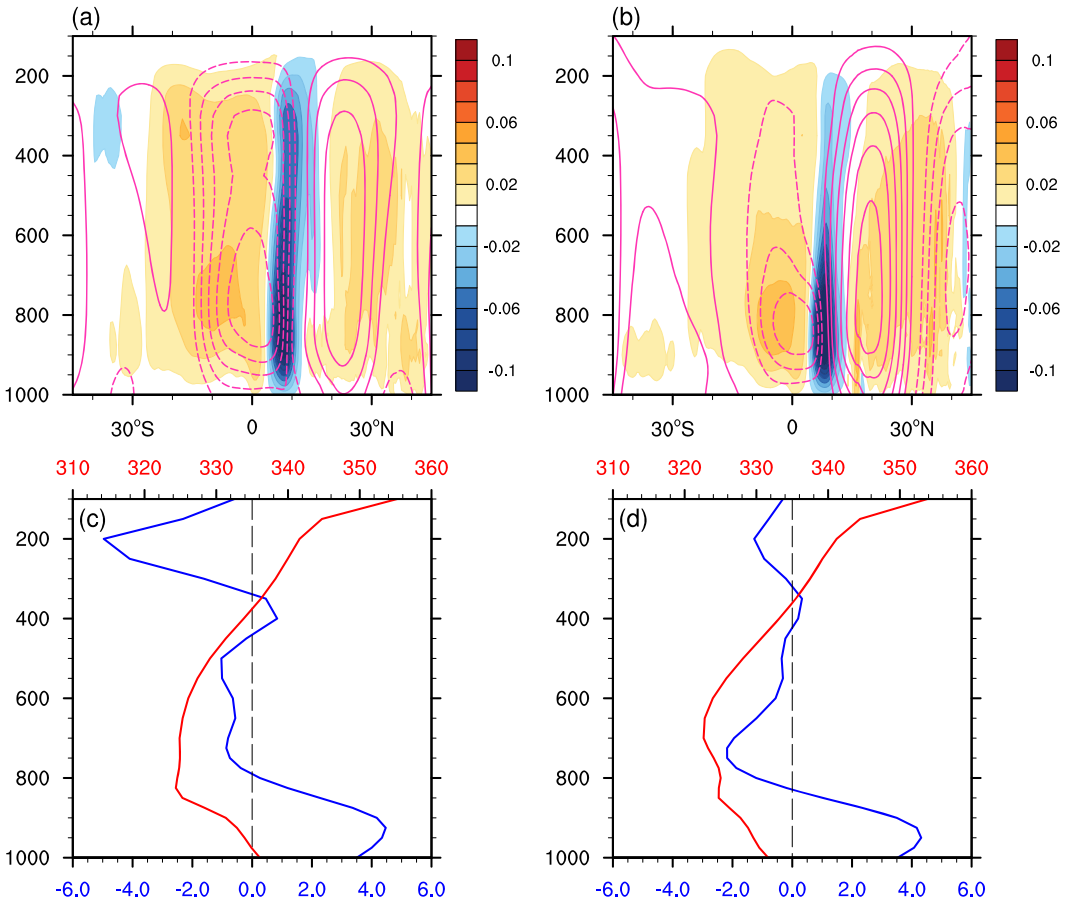

Figure 4. Sector mean meridional mass streamfunction (contour, interval 10^{10} kg s^{-1}) for 15 days (3 pentads) average around (a) 15–19 June and (b) 17–21 November in the Eastern Pacific sector. Solid (dashed) maroon contours indicate positive (negative) values. Positive (negative) contours indicate northward (southward) meridional flow at upper levels, and oppositely directed flows at levels below the streamfunction maximum (minimum). The shading shows vertical pressure velocity (Pa s^{-1}). (c, d) Vertical profiles of the MSE (red, K) and meridional wind (blue, m s^{-1}) at the equator for 15 days average around (c) 15–19 June and (d) 17–21 November. The vertical dashed line indicates zero value for wind speed.

at upper levels. This results in a distorted cell boundary, which resides in the NH up to around 700 hPa, and in the SH at lower pressures. This structure explains both the ITCZ and the EFE positions: strongly tied to the lower-level convergence, the precipitation maximum is colocated with the cell boundary in the lower troposphere (Figure 2d). The cell meridional energy transport and the EFE instead are influenced by the overall vertical circulation structure. In particular, the development of a shallow return flow at the equator near the level of minimum MSE and the northward flow at upper levels favor energy transport in the direction of the lower-level flow and, hence, a negative GMS between the ITCZ in the NH and the EFE in the SH (Figure S6a).

It is important to emphasize how this structure, while explaining how the required energy transport is achieved in the zonal mean, is not representative of a dominant structure at all longitudes, but arises from different circulation structures in different sectors. The distorted boundary between the two Hadley cells in fact results from a more bottom-heavy overturning cell in the Eastern Pacific sector with ascending motion in the NH, and a more top-heavy overturning cell with ascending motion in the SH and near the equator over the Western Pacific and Indian sectors (Figure S5).

3.2. Eastern Pacific Sector

Previous work has highlighted how shallow and deep Hadley cell modes coexist in the Eastern Pacific ITCZ (Zhang et al., 2004). The deep mode is associated with a return flow in the upper troposphere, while the

shallow mode features a return flow across the equator near 850 hPa. The latter is most prominent in convectively suppressed cases and strongest in boreal fall and winter, but it tends to persist throughout the year and imprints on the structure of the sector-mean Hadley cell. Building on this work, here we further analyze seasonal changes in the circulation vertical structure and we explore how it influences its GMS in relation to the ITCZ position. In the Eastern Pacific sector (150°W to 90°W, indicated within the black vertical lines in Figure 1), the precipitation stays in the NH throughout the year while a secondary ITCZ develops in the SH between February and May, reaching its maximum in April (Figure 3a). The ITCZ in the NH has a temporally asymmetric evolution, being stronger as the ITCZ is expanding to the north than as it is retreating to the south. Given that, similar to what is seen in the zonal mean, the ITCZ does not evolve at the same frequency as the annual cycle of insolation, the temporal relationship between the EFE and the ITCZ cannot simply be described as a lag. At two pentads with the same ITCZ position but different EFEs (June and November pentads, indicated by the vertical black dashed lines in Figure 3), the cross-equatorial cell corresponds to very different energy transports. In the June pentad, the expanding cross-equatorial cell transports energy across the equator to the south, while the cross-equatorial cell in the November pentad tends to transport some energy to the north, which corresponds to negative GMS (Figure S6b).

Figure 4 shows the overturning cell structure for the two different pentads. While there is evidence that the shallow mode persists throughout the year (e.g., Back & Bretherton, 2006; Zhang et al., 2004), we do see differences in the circulation structure between the expanding and retreating phases. More specifically, in the expanding phase, the shallow return flow extends over a deeper layer within the midtroposphere between around 800 and 450 hPa, and there exists a strong return flow at upper levels. This results in energy being transported in the same direction as the upper-level flow (Figures 4a, 4c, and S6b). The retreating cross-equatorial cell, however, has a shallower structure, with stronger shallow return flow and, more importantly, a much weaker flow at upper levels, which results in an overturning circulation and vertical velocity that have clear bottom-heavy vertical profiles (Figures 4b and 4d). This clear bottom heaviness is what favors a more negative GMS at this time of the year near the equator (Figure S6b).

To explore the possible reasons for these seasonal differences in the overturning cell structure, the evolutions of the surface temperature, its Laplacian, and lower-level divergence are calculated (Figures 3c–3e). We find that the SSTs are much weaker and their Laplacian and lower-level convergence are much stronger near the ITCZ as it is retreating from the NH around November. This is consistent with arguments by Back and Bretherton (2009) and Lindzen and Nigam (1987), which link a more negative SST Laplacian and weaker SSTs to more bottom-heavy convection due to the corresponding stronger lower-level convergence and hindrance to the development of top-heavy convective profiles.

4. Discussions and Conclusions

In this study, we have analyzed the seasonal evolution of the ITCZ, the structure of the overturning circulation in which the ITCZ is embedded, and their relationship to energetic variables. While the EFE and the ITCZ tend to coevolve during the seasonal cycle, there is a clear offset between the two, with strong zonal variations. Similarly to what we proposed in Wei and Bordoni (2018), the EFE and the ITCZ on seasonal and shorter timescales respond differently to the seasonal cycle of insolation and are not necessarily colocated. More specifically, the required energy balance is not always achieved through the Hadley cell shifting its ascending branch to follow the EFE, but through changes in the efficiency of its energy transport. This pathway allows commonly held relationships between the ITCZ, EFE, and cross-equatorial energy transport to break down on seasonal and shorter timescales.

While in the idealized simulations the temporal relationship between the ITCZ and the EFE can be described as a lag (Wei & Bordoni, 2018), in observations, this relationship is complicated by the fact that both the ITCZ and the EFE do not evolve just following the period of the annual harmonic. However, a clear offset exists, raising the question as to how the required energy balance is achieved as the EFE and the ITCZ reside on opposite sides of the equator or when the energy flux distribution is not monotonic around the EFE.

In the global zonal mean, the ITCZ resides in the NH for most of the seasonal cycle, while the EFE spends around equal times in both hemispheres. As the EFE retreats from the NH to the SH, while the ITCZ remains north of the equator, the associated Hadley circulation must transport energy in the direction of its lower rather than its upper branch, which is associated with a negative GMS. This occurs as the Hadley cell develops a bottom-heavy structure, with a distorted dividing boundary between the northern and southern Hadley

cells, which is in the NH at lower levels and in the SH at upper levels. This results in a shallow meridional return flow at the equator that favors a southern cell with negative GMS. This Hadley cell structure results from strong zonal differences in the overturning structure, with a bottom-heavy cross-equatorial cell with ascending branch in the NH over the Eastern Pacific and a deeper overturning with ascending branch in the SH over other sectors, such as the Indian and Western Pacific sectors. While bottom-heavy convection exists most of the time throughout the year in the Eastern Pacific, the bottom heaviness at times at which the ITCZ migrates from the Northern to the Southern Hemisphere is much stronger, favoring a more negative GMS at these times. This stronger bottom heaviness seems to be associated with weaker SSTs and stronger SST Laplacian in the Eastern Pacific sector.

It is important to note how estimates of the position of the EFE and cross-equatorial energy transport from reanalyses, energetic quantities that have been theoretically linked to the ITCZ position, are extremely sensitive to how and which budgets are closed. For instance, the zonal and annual mean cross-equatorial energy transport is zero if we perform a barotropic adjustment on the dry mass budget, but is −0.23 PW if we perform the adjustment to close the MSE budget. This highlights difficulties in closing the MSE budget from reanalyses and suggests that conclusions based on energetic arguments need to be interpreted with caution. Additionally, while it has been shown that reanalyses tend to overestimate the shallow convection in the Eastern Pacific sector (e.g., Huaman & Takahashi, 2016), MERRA-2 performs better than other reanalysis products (Huaman & Schumacher, 2018), giving us confidence on the robustness of the results reported here.

Due to the complexities existing in reanalysis data, the gap between them and the idealized simulations that inspired this investigation is large. It will be useful to conduct simulations that, by progressively increasing complexity, can provide understanding of processes that control the seasonal cycle of the ITCZ and its relation to energetic constraints.

Data Availability Statement

The data were originally downloaded from NASA MERRA-2 website (https://gmao.gsfc.nasa.gov/reanalysis/MERRA‐2/) and the dry mass and MSE adjusted data are available online (https://data.caltech.edu/records/1421).

Acknowledgments
This work was supported by the National Science Foundation (AGS-1462544). We thank Ori Adam, Andy Ingersoll, Tapio Schneider, Andrew Thompson, and Joao Teixeira for helpful discussion.

References

Adam, O., Bischoff, T., & Schneider, T. (2016a). Seasonal and interannual variations of the energy flux equator and ITCZ. Part I: Zonally averaged ITCZ position. *Journal of Climate*, *29*(9), 3219–3230. https://doi.org/10.1175/JCLI-D-15-0512.1

Adam, O., Bischoff, T., & Schneider, T. (2016b). Seasonal and interannual variations of the energy flux equator and ITCZ. Part II: Zonally varying shifts of the ITCZ. *Journal of Climate*, *29*(20), 7281–7293. https://doi.org/10.1175/JCLI-D-15-0710.1

Back, L. E., & Bretherton, C. S. (2006). Geographic variability in the export of moist static energy and vertical motion profiles in the tropical pacific. *Geophysical Research Letters*, *33*, L17810. https://doi.org/10.1029/2006GL026672

Back, L. E., & Bretherton, C. S. (2009). A simple model of climatological rainfall and vertical motion patterns over the tropical oceans. *Journal of Climate*, *22*(23), 6477–6497. https://doi.org/10.1175/2009JCLI2393.1

Biasutti, M., & Voigt, A. (2020). Seasonal and CO_2-induced shifts of the ITCZ: Testing energetic controls in idealized simulations with comprehensive models. *Journal of Climate*, *33*, 2853–2870.

Bischoff, T., & Schneider, T. (2014). Energetic constraints on the position of the intertropical convergence zone. *Journal of Climate*, *27*(13), 4937–4951. https://doi.org/10.1175/JCLI-D-13-00650.1

Bischoff, T., & Schneider, T. (2016). The equatorial energy balance, ITCZ position, and double-ITCZ bifurcations. *Journal of Climate*, *29*(8), 2997–3013. https://doi.org/10.1175/JCLI-D-15-0328.1

Bosilovich, M., Akella, S., Coy, L., Cullather, R., Draper, C., Gelaro, R., et al. (2015). MERRA-2: Initial evaluation of the climate, *NASA Tech. Rep. Series on Global Modeling and Data Assimilation*, NASA/TM–2015-104606 (Vol. 43, 139 pp.).

Donohoe, A., Marshall, J., Ferreira, D., Armour, K., & McGee, D. (2014). The interannual variability of tropical precipitation and interhemispheric energy transport. *Journal of Climate*, *27*(9), 3377–3392. https://doi.org/10.1175/JCLI-D-13-00499.1

Donohoe, A., Marshall, J., Ferreira, D., & McGee, D. (2013). The relationship between ITCZ location and cross-equatorial atmospheric heat transport: From the seasonal cycle to the last glacial maximum. *Journal of Climate*, *26*(11), 3597–3618. https://doi.org/10.1175/JCLI-D-12-00467.1

Emanuel, K. A. (1995). On thermally direct circulations in moist atmospheres. *Journal of the Atmospheric Sciences*, *52*(9), 1529–1534. https://doi.org/10.1175/1520-0469(1995)052<1529:OTDCIM>2.0.CO;2

Feldl, N., & Bordoni, S. (2016). Characterizing the Hadley circulation response through regional climate feedbacks. *Journal of Climate*, *29*(2), 613–622. https://doi.org/10.1175/JCLI-D-15-0424.1

Frierson, D. M. W. (2007). The dynamics of idealized convection schemes and their effect on the zonally averaged tropical circulation. *Journal of the Atmospheric Sciences*, *64*(6), 1959–1976. https://doi.org/10.1175/JAS3935.1

Frierson, D. M. W., & Hwang, Y.-T. (2012). Extratropical influence on ITCZ shifts in slab ocean simulations of global warming. *Journal of Climate*, *25*(2), 720–733. https://doi.org/10.1175/JCLI-D-11-00116.1

Frierson, D. M. W., Hwang, Y.-T., Fučkar, N. S., Seager, R., Kang, S. M., Donohoe, A., et al. (2013). Contribution of ocean overturning circulation to tropical rainfall peak in the Northern Hemisphere. *Nature Geoscience*, *6*(10), 1–5. https://doi.org/10.1038/ngeo1987

Hill, S. A., Ming, Y., & Held, I. S. (2015). Mechanisms of forced tropical meridional energy flux change. *Journal of Climate*, *28*(5), 1725–1742. https://doi.org/10.1175/JCLI-D-14-00165.1

Hill, S. A., Ming, Y., Held, I. M., & Zhao, M. (2017). A moist static energy budget–based analysis of the Sahel rainfall response to uniform oceanic warming. *Journal of Climate*, *30*(15), 5637–5660. https://doi.org/10.1175/JCLI-D-16-0785.1

Huaman, L., & Schumacher, C. (2018). Assessing the vertical latent heating structure of the East Pacific ITCZ using the CloudSat CPR and TRMM PR. *Journal of Climate*, *31*(7), 2563–2577. https://doi.org/10.1175/JCLI-D-17-0590.1

Huaman, L., & Takahashi, K. (2016). The vertical structure of the Eastern Pacific ITCZs and associated circulation using the TRMM precipitation radar and in situ data. *Geophysical Research Letters*, *43*, 8230–8239. https://doi.org/10.1002/2016GL068835

Hwang, Y.-T., Frierson, D. M. W., & Kang, S. M. (2013). Anthropogenic sulfate aerosol and the southward shift of tropical precipitation in the late 20th century. *Geophysical Research Letters*, *40*, 2845–2850. https://doi.org/10.1002/grl.50502

Kang, S. M., Frierson, D. M. W., & Held, I. M. (2009). The tropical response to extratropical thermal forcing in an idealized GCM: The importance of radiative feedbacks and convective parameterization. *Journal of the Atmospheric Sciences*, *66*(9), 2812–2827. https://doi.org/10.1175/2009JAS2924.1

Kang, S. M., Held, I. M., Frierson, D. M. W., & Zhao, M. (2008). The response of the ITCZ to extratropical thermal forcing: Idealized slab-ocean experiments with a GCM. *Journal of Climate*, *21*(14), 3521–3532. https://doi.org/10.1175/2007JCLI2146.1

Lindzen, R. S., & Nigam, S. (1987). On the role of sea surface temperature gradients in forcing low-level winds and convergence in the tropics. *Journal of the Atmospheric Sciences*, *44*(17), 2418–2436. https://doi.org/10.1175/1520-0469(1987)044<2418:OTROSS>2.0.CO;2

Marshall, J., Donohoe, A., Ferreira, D., & McGee, D. (2013). The ocean's role in setting the mean position of the inter-tropical convergence zone. *Climate Dynamics*, *42*(7-8), 1967–1979. https://doi.org/10.1007/s00382-013-1767-z

McGee, D., Donohoe, A., Marshall, J., & Ferreira, D. (2014). Changes in ITCZ location and cross-equatorial heat transport at the Last Glacial Maximum, Heinrich Stadial 1, and the mid-Holocene. *Earth and Planetary Science Letters*, *390*, 69–79. https://doi.org/10.1016/j.epsl.2013.12.043

Merlis, T. M., Schneider, T., Bordoni, S., & Eisenman, I. (2013). The tropical precipitation response to orbital precession. *Journal of Climate*, *26*(6), 2010–2021. https://doi.org/10.1175/JCLI-D-12-00186.1

Privé, N. C., & Plumb, R. A. (2007). Monsoon dynamics with interactive forcing. Part I: Axisymmetric studies. *Journal of the Atmospheric Sciences*, *64*(5), 1417–1430. https://doi.org/10.1175/JAS3916.1

Rencurrel, M. C., & Rose, B. E. J. (2020). The efficiency of the Hadley cell response to wide variations in ocean heat transport. *Journal of Climate*, *33*(5), 1643–1658.

Rienecker, M. M., Suarez, M. J., Gelaro, R., Todling, R., Bacmeister, J., Liu, E., et al. (2011). MERRA: NASA's modern-era retrospective analysis for research and applications. *Journal of Climate*, *24*(14), 3624–3648. https://doi.org/10.1175/JCLI-D-11-00015.1

Schneider, T., Bischoff, T., & Haug, G. H. (2014). Migrations and dynamics of the intertropical convergence zone. *Nature*, *513*(7516), 45. https://doi.org/10.1038/nature13636

Seo, J., Kang, S. M., & Merlis, T. M. (2017). A model intercomparison of the tropical precipitation response to a CO_2 doubling in aquaplanet simulations. *Geophysical Research Letters*, *44*, 993–1000. https://doi.org/10.1175/2009JCLI3049.1

Trenberth, K. E. (1991). Climate diagnostics from global analyses: Conservation of mass in ECMWF analyses. *Journal of Climate*, *4*(7), 707–722. https://doi.org/10.1175/1520-0442(1991)004<0707:CDFGAC>2.0.CO;2

Trenberth, K. E., & Caron, J. M. (2001). Estimates of meridional atmosphere and ocean heat transports. *Journal of Climate*, *14*(16), 3433–3443. https://doi.org/10.1175/1520-0442(2001)014<3433:EOMAAO>2.0.CO;2

Voigt, A., Biasutti, M., Scheff, J., Bader, J., Bordoni, S., Codron, F., et al. (2016). The tropical rain belts with an annual cycle and a continent model intercomparison project: TRACMIP. *Journal of Advances in Modeling Earth Systems*, *8*, 1868–1891. https://doi.org/10.5194/gmd-2016-69

Wei, H.-H., & Bordoni, S. (2018). Energetic constraints on the ITCZ position in idealized simulations with a seasonal cycle. *Journal of Advances in Modeling Earth Systems*, *10*, 1708–1725. https://doi.org/10.1029/2018MS001313

Zhang, C., McGauley, M., & Bond, N. A. (2004). Shallow meridional circulation in the tropical eastern Pacific. *Journal of Climate*, *17*(1), 133–139. https://doi.org/10.1175/1520-0442(2004)017<0133:SMCITT>2.0.CO;2